Proceedings of the 3rd IEEE International
Conference on Micro/Nano Sensors for AI, Healthcare and Robotics
March 2 - 3, 2024, Shenzhen, China

2024 IEEE 3rd International Conference on Micro/Nano Sensors for AI, Healthcare, and Robotics (NSENS) | 979-8-3503-7521-3/24/$31.00 ©2024 IEEE | DOI: 10.1109/NSENS62142.2024.10561418

A Hybrid Deep Learning Approach for Cuff-less Noninvasive Continuous Blood Pressure Estimation Based on Photoplethysmography

Md Sadek Ali, Md Shohidul Islam, Raymond Hon-Fu Chan, Kannie Wai Yan Chan, and Derek Ho*

Abstract— **Conventional deep learning architectures do not adequately address the requirements of wearable high-precision medical devices such as blood pressure (BP) monitors. This paper presents a novel hybrid deep learning architecture that leverages advancements in sensors and signal processing modules for cuffless and continuous BP monitoring devices, emphasizing enhanced precision in an energy constrained system. The proposed architecture comprises a combination of a convolutional neural network and a bidirectional gated recurrent unit. The proposed model adopts a data-driven end-to-end approach to directly process raw photoplethysmography (PPG) signals, enabling simultaneous estimation of systolic BP and diastolic BP without the need for feature extraction. Performance evaluation was conducted using the Multiparameter Intelligent Monitoring in Intensive Care II dataset, yielding small mean errors of 0.664 mmHg and -0.028 mmHg for the estimated and reference SBP and DBP, respectively.**

I. Introduction

Cuffless and noninvasive blood pressure (BP) measurement has garnered significant attention and has made substantial advancements in recent decades. Many of these approaches rely on photoplethysmography (PPG) and electrocardiography (ECG). One extensively studied approach is pulse transit time (PTT) [1-2]. However, PTT often exhibits an inverse correlation with BP [3]. Another well-known cuffless approach is pulse arrival time (PAT) [4]. This technique involves estimating the time delay between the R peak of the ECG waveform and a specific point on the ascending edge of a distal PPG waveform [5]. Notwithstanding their advantages, both PTT and PAT methods have notorious implementation challenges, namely the requirement for concurrent measurement of signals at two distinct body sites, necessitating the use of two sensors (ECG and PPG) to record the input signals for parameter estimation. This requirement can be inconvenient or even prohibitive for certain patients. Moreover, incorporating multiple sensors increases the requirement for signal pre-processing, which not only consumes time but also introduces additional computational complexity to the process. In recent research, there has been a surge of interest in using PPG as a single measurement sensor for BP estimation. This approach has been gaining popularity due to its simplicity and capability to enable cuffless and continuous BP measurements. PPG is an optical sensor technology that combines a light-emitting diode (LED) with a photodetector (PD) [6]. This sensor is not only cost-effective but can also be readily integrated into wearable devices. PPG is considered a vital physiological signal as it offers insights into the function and health of the cardiovascular system. For example, there is a correlation between peripheral volumetric changes in blood vessels and BP [7]. This correlation allows for the utilization of specific PPG features to predict systolic BP (SBP) and diastolic BP (DBP) employing machine learning (ML) or deep learning (DL) algorithms. Despite the above capabilities, nonetheless, the relationship between these PPG features and BP is not direct and continuous [8]. Estimating BP using PPG heavily depends on signal preprocessing, obtaining significant features, and utilizing ML approaches to establish the correlation between these extracted features and blood pressure.

Several recent advancements have been reported. Kachuee et al. [9] developed a system utilizing PTT for the cuffless and continuous BP prediction and mean arterial pressure. This system incorporated multiple ML techniques and utilized both PPG and ECG signals. The implementation of this approach involved meticulous signal preprocessing and intricate steps for feature extraction. Hasanzadeh et al. [10] conducted a study where they extracted PPG morphological features and employed various ML algorithms to predict SBP and DBP. Nevertheless, the evaluation outcomes indicated significant prediction errors for both SBP and DBP, and this approach did not adhere to global standards set by organizations like the American Association for Medical Instrumentation (AAMI) [11] and the British Hypertension Society (BHS) [12]. Consequently, the system showed limited capability for accurate cuffless BP monitoring and lacked generalizability.

M. S. Ali and M. S. Islam contributed equally to this work.

M. S. Ali and M. S. Islam are with the Hong Kong Centre for Cerebro-cardiovascular Health Engineering (COCHE), Hong Kong, China (e-mail: msali@hkcoche.org, mdsislam@hkcoche.org).

R. HF. Chan is with the Department of Mathematics, City University of Hong Kong, and Hong Kong Centre for Cerebro-cardiovascular Health Engineering (COCHE), Hong Kong, China (e-mail: raymond.chan@cityu.edu.hk).

K. W. Y. Chan is with the Department of Biomedical Engineering, City University of Hong Kong, and Hong Kong Centre for Cerebro-cardiovascular Health Engineering (COCHE), Hong Kong, China (e-mail: kanniew.y.c@cityu.edu.hk).

*D. Ho is with the Department of Materials Science and Engineering, City University of Hong, and Hong Kong Centre for Cerebro-cardiovascular Health Engineering (COCHE), Hong Kong, China (corresponding author e-mail: derekho@cityu.edu.hk).

979-8-3503-7521-3/24/$31.00 ©2024 IEEE

Gupta [13] utilized various ML algorithms to estimate SBP and DBP by incorporating higher-order derivative features of the PPG signal. The authors demonstrated that these additional nonlinear features improved the accuracy of estimation, albeit with increased computational costs.

All of the aforementioned approaches possess their own advantages and disadvantages. One notable advantage is their ability to predict BP utilizing a single PPG sensor without the need for a cuff, making it a simple and cost-effective method. However, there are certain limitations to consider. Due to the lack of consistent linearity between BP and PPG features, linear models are not suitable for accurately capturing this relationship when assessed on a diverse dataset acquired from a large and varied population. In contrast, classical ML models such as support vector machines (SVM) and random forest tend to exhibit better precision in such scenarios. It is worth noting that separate models need to be established for SBP and DBP prediction when using these algorithms. However, it is beneficial to model SBP and DBP simultaneously using a single model architecture, as DBP is strongly correlated with SBP and can enhance its estimation. Neural networks offer a solution to this challenge by leveraging large datasets more efficiently and precisely compared to traditional ML algorithms. However, not all neural network models are suitable for this task. Some neural network models are specifically developed to handle time series data for long-term estimate, while others, such as non-recurrent neural networks, solely estimate the output based on the current input vector without considering its historical context. Consequently, non-recurrent neural networks do not effectively capture the temporal variations in the PPG features, leading to a gradual degradation in prediction accuracy over time.

In recent times, significant progress has been made in the field of BP measurement by employing sophisticated models that utilize big data and neural networks. Xing et al. [14] applied fast Fourier transformation (FFT) to extract features in frequency domain from the PPG signal, in contrast to the time domain features used in previous approaches, for BP estimation. They employed a feedforward artificial neural network (ANN) for this purpose. However, they reported that relying solely on these features was insufficient for achieving accurate BP estimation. Yao et al. [15], demonstrated a portable BP estimation system using a two-layer ANN approach that incorporated multidimensional feature fusion. The authors aimed to enhance the accuracy of BP estimation. However, the complex feature extraction process resulted in high computational complexity, which limited the real-time application of wearable healthcare devices. El-Hajj et al. [16] developed attention mechanism assisted two DL models using bidirectional long short-term memory (BiLSTM) and bidirectional gated recurrent unit (BiGRU). These models were employed for the estimation of SBP and DBP with 22 characteristic features extracted by complicated feature engineering. The performance of these models was found to be satisfactory and aligned with the standards set by the AAMI. However, another limitation of the approach was that the authors developed two separate models, which restricted their deployment in low-complexity wearable devices. In their study, Yang et al. [17] introduced a hybrid DL model that combines convolutional neural networks (CNN) and LSTM networks to estimate BP. This model leverages both PPG and ECG raw signals, as well as participant-specific physical characteristics like age, height, weight, and gender. However, the utilization of multi-modal signals in the model increases the computational complexity of the prediction model and raises the cost of hardware implementation.

In this paper, we present a data-driven, end-to-end approach for the estimation of BP, utilizing a hybrid DL architecture called CNN-BiGRU, which only requires the PPG signal as input. The proposed framework eliminates the need for explicit features and achieves end-to-end BP estimation. The CNN component extracts relevant features from the raw PPG signal, while the BiGRU network captures sequential dependencies in the data. To the best of our knowledge, no prior research has been reported for simultaneous estimation of SBP and DBP using a deep learning approach with the CNN-BiGRU architecture. The main contribution of this work lies in the architectural development of a hybrid DL model that combines CNN and recurrent neural network (RNN) for accurate BP estimation based on PPG signals.

The rest of the paper is presented as follows: Section II presents employed materials and proposed methodological workflow, Section II stretches the evaluation results and analysis, and Section IV concludes the paper while outlining imminent works.

II. Materials and Methods

This section describes the employed dataset and its preprocessing steps and the proposed deep learning model. To provide a visual overview of the methodology, Fig. 1 depicts a workflow diagram.

A. Dataset and Signal Preprocessing

The proposed DL model undergoes training and testing using the University of California, Irvine (UCI) Machine Learning Repository dataset. This dataset is extracted from the publicly available "Multi-parameter Intelligent Monitoring in Intensive Care (MIMIC-II)" database, which can be accessed through the Physionet repository [18]. The MIMIC-II database contains simultaneous recordings of various parameters from patients in the intensive care unit (ICU), including physiological signals and physiological parameters. For this study, we have extracted simultaneous recordings of PPG, and arterial BP (ABP) from 6000 subjects, which are provided in the UCI repository. The sampling frequency for these signals is set at 125 Hz with 8-bit precision. To leverage the recurrent neural network's capability for handling time series data, both the PPG signals and their associated ABP references are segmented into 5.6-second windows (i.e., 700 samples). To enhance the dataset's reliability, additional refinement steps are implemented. Specifically, segments with unreliable ABP

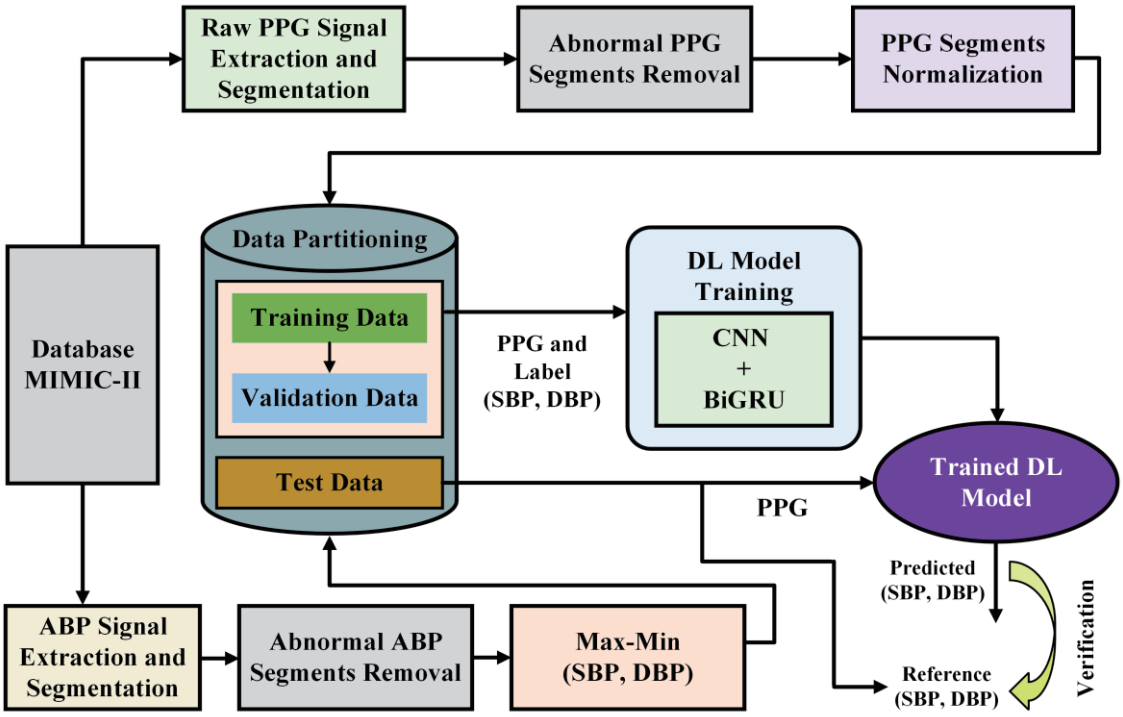

Figure 1. Methodological workflow of the proposed deep learning-based BP estimation system.

and its corresponding PPG are excluded. Segments with excessively high or low values of BP, such as SBP greater than or equal to 180, SBP less than or equal to 100, DBP greater than or equal to 100, and DBP less than or equal to 55, are removed. This refinement process results in the total number of considered segments 184,040. The reference scores for SBP and DBP are calculated using the ABP signal segments, applying the max-min approach. Lastly, the amplitude of the PPG signal is normalized using min-max normalization [16], ensuring that the values are scaled to fall within the range of [0,1].

B. Proposed DL Model for BP Estimation

The proposed DL architecture adopts a two-level hierarchy model that incorporates stacked CNN, and bidirectional RNN. Fig. 2 illustrates the topological structure of the developed DL model. In the lower hierarchy level, CNN is utilized to automatically extract essential features from the input raw PPG signal. Moving to the upper level, RNN is designed using two BiGRU layers to capture the temporal relationships among the extracted features and make predictions. Each segment of the PPG signal serves as input for the CNN layer. The output from the CNN block is subsequently passed to the BiGRU layers, which simultaneously predict both SBP and DBP.

The CNN block comprises of three 1D convolutional layers, with a rectified linear unit (ReLU) activation function, batch normalization (BN), and 1D maxpooling for each layer. The output of the final maxpooling layer in the CNN block is then used as input for the prediction module. The ReLU activation function is chosen due to its faster training speed compared to other activation functions. Additionally, batch normalization is applied after each convolutional layer to enhance the model's generalization capability. The max-pooling operation facilitates the extraction of combined features by aggregating relevant information from neighboring data points. Consequently, the CNN components serve as an effective automatic feature extractor.

The BP estimation network is constructed by stacking two BiGRU layers using the "concat" merge-mode. Each BiGRU layer consists of a forward GRU layer and a backward GRU layer. The GRU is another form of the LSTM that controls information flow through multiple gating mechanisms [16]. However, unlike LSTM, the GRU's hidden state comprises only two gates and does not have an additional memory cell. Consequently, the GRU is a simplified variant of LSTM that requires fewer computational resources. By connecting the input sequence with its reverse copy, the BiGRU network enhances its ability to capture longer dependencies, resulting in improved model performance. The "concat" merge-mode ensures that all data from both the forward input sequence and its reverse copy is preserved, preventing any loss of information. This enables the network to effectively discern which information is relevant for robust loss minimization during training. The output of the final BiGRU layer is then flattened and used as input for two dense layers, followed by the ReLU activation function, to generate estimated SBP and DBP values. To prevent the model from becoming overly specific to the training sequence, a dropout layer with a probability factor of 0.1 is applied after each BiGRU layer. This inclusion promotes network robustness and helps

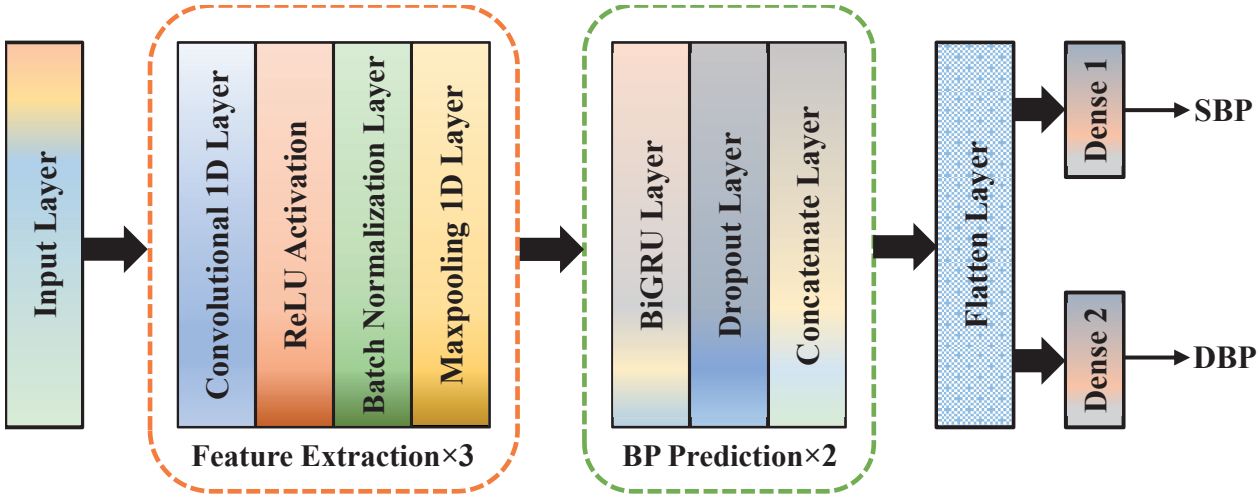

Figure 2. Topological structure of the proposed deep learning model.

eradicate the issue of overfitting. For the sake of brevity, we exclude the detailed structures and parameters of the proposed model in this presentation.

C. Model Training and Evaluation

The dataset for this study is partitioned into three sets: 80% for training, 10% for validation, and 10% for evaluation. The validation set plays a crucial role in selecting the best optimized model. During training, a batch size of 64 is utilized, and the model is trained with early stopping for a maximum of 50 epochs and a learning rate of 0.5. Through empirical investigation, it has been determined that the Adam optimizer [19] outperformed other optimizers, providing superior and more consistent performance. The mean squared error (MSE) is utilized as the loss function during training.

III. Results and Analysis

The performance evaluation of the proposed DL model is carried out by averaging the model scores across all testing sets. In this assessment, mean error (ME), mean absolute error (MAE), root mean squared error (RMSE), standard deviation (SD), and Pearson's correlation coefficients are utilized as effective metrics for estimation tasks.

A. Evaluation Results

The performance results of the proposed DL model on the MIMIC-II dataset are presented in Table I. The architecture of the model utilizes CNN-GRU units to achieve simultaneous estimation of SBP and DBP, with average ME, MAE, RMSE, and SD values of 0.318, 3.894, 6.262 and 4.902, respectively. Additionally, a comparison study is conducted between the ground truth scores and the predicted scores of SBP and DBP, as depicted in Fig. 3. The graph in Fig. 3 (A) illustrates the comparison between the reference and predicted scores for SBP, while the graph in Fig. 3 (B) shows the comparison between the reference DBP values and the predicted values for 100 test data points, with each data point comprising 700 samples. The inference graphs for both SBP and DBP exhibit a good agreement between the reference and estimated values. Notably, the proposed architecture, utilizing GRU units, demonstrates lower estimation errors compared to CNN-LSTM units [17]. Figure 4 (A) and (B) display a statistical analysis of the estimation error between the reference and

TABLE I. Performance of the Proposed CNN-BiGRU DL Model

Parameter	ME (mmHg)	MAE (mmHg)	RMSE (mmHg)	±SD (mmHg)
SBP	0.664	4.852	7.909	6.245
DBP	-0.028	2.937	4.615	3.560

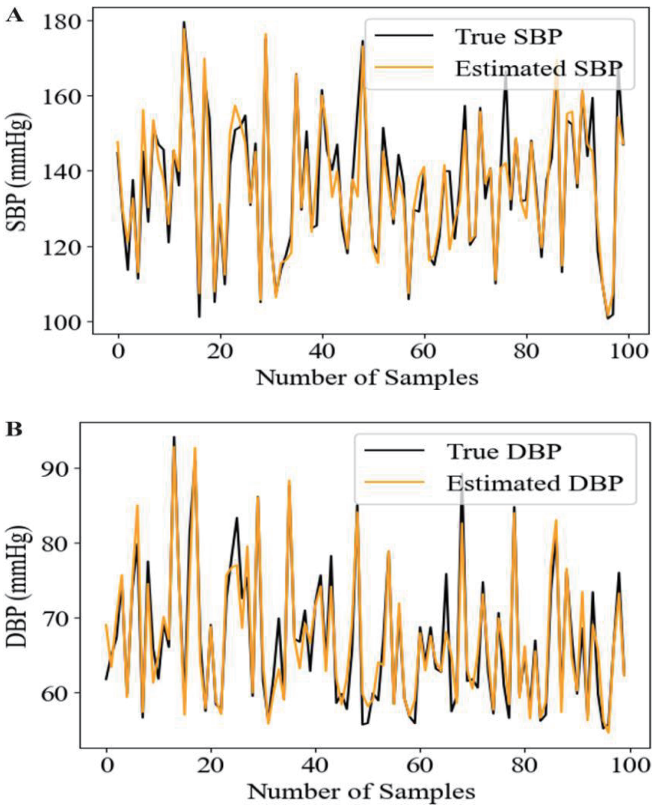

Figure 3. Graphical comparison between reference and predicted scores of 100 test data points. (A) SBP and (B) DBP.

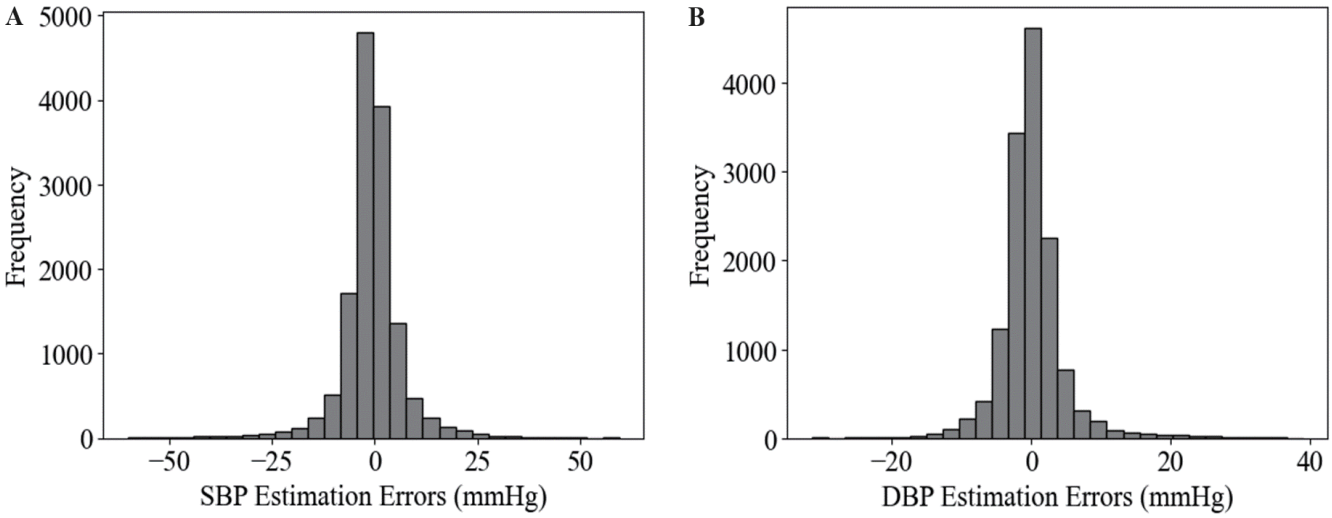

Figure 4. illustration of errors between reference and predicted values along with corresponding histograms. (A) SBP, and (B) DBP.

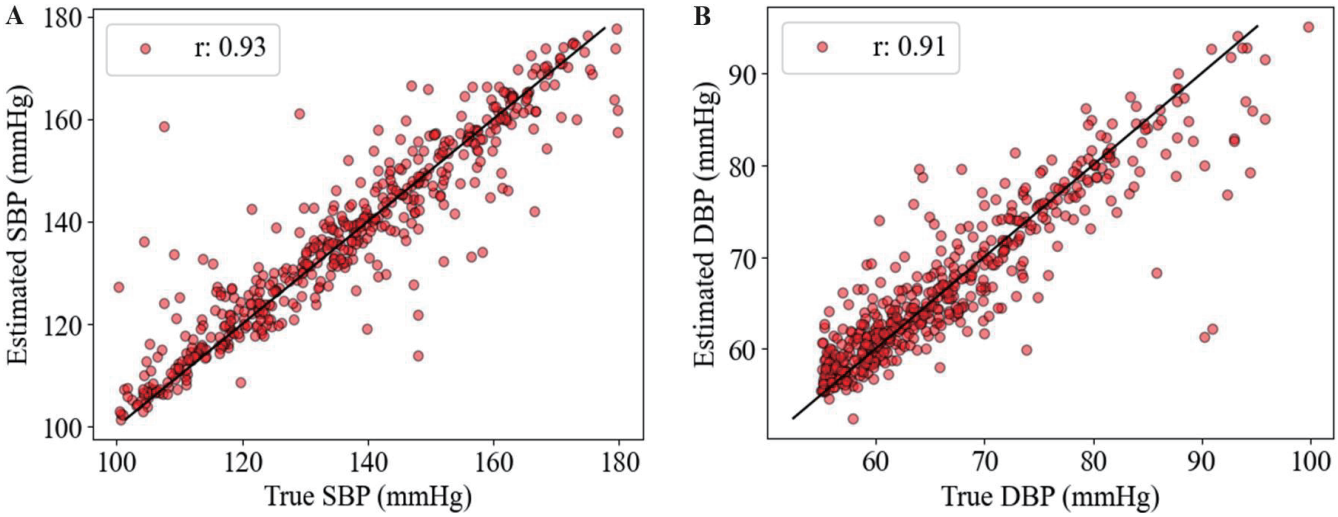

Figure 5. The correlation graph between the reference and estimated values. The Pearson's correlation coefficient (*r)* values of (A) SBP, and (B) DBP are 0.93 and 0.91, respectively.

predicted values of SBP and DBP, respectively, in the form of error histograms. The histograms reveal that the prediction errors for both SBP and DBP approximate a normal distribution centered around zero. The scale of the error distribution is relatively narrow, spanning approximately [-25, 25] for SBP and [-15, 15] for DBP. Notably, the error distribution of SBP is greater than 1.5 times wider than that of DBP, which reflects the broader range of SBP values.

In Fig. 5 (A) and (B), the linear correlation analysis provides further insight into the relationship between the estimated values and the ground truth BP values. The analysis reveals a strong correlation between the estimations and the reference values for both SBP and DBP. The Pearson's coefficient (*r*) values are used to quantify the strength of the correlation. In this case, an *r* value of 0.93 is obtained for the correlation between the estimations and the reference SBP values, indicating a strong positive correlation. Similarly, the correlation between the estimations and the reference DBP values yields an *r* value of 0.91, indicating a strong positive correlation as well. It signifies that the proposed model is effective in accurately estimating blood pressure, as evidenced by the strong relationship between the estimated values and the label values.

B. Comparison with International Standards

In our study, we have conducted a comprehensive analysis to validate the efficiency of our proposed DL architecture for simultaneously estimating SBP and DBP from the raw PPG signal. We have compared our evaluation results with the established criteria set by AAMI and BHS standards. The AAMI standard requires an evaluation framework that involves a minimum of 85 subjects. It assesses the accuracy of the algorithm by examining the ME and SD, which should fall

TABLE II: PERFORMANCE COMPARISON WITH THE BHS STANDARD

	BHS Grade/ Physiological Parameters	Cumulative Error Percentage			Achieved Grade
		≤ 5 (mmHg)	≤ 10 (mmHg)	≤ 15 (mmHg)	-
BHS	A	60	85	95	-
	B	50	75	90	-
	C	40	65	85	-
This work	SBP	70.16	88.52	94.16	A
	DBP	84.38	95.60	98.26	A

TABLE III: PERFORMANCE COMPARISON WITH THE AAMI STANDARD

	Physiological Parameters	No. of Subjects	ME (mmHg)	SD (mmHg)
AAMI	SBP and DBP	≥ 85	≤ 5	≤ 8
This work	SBP	6000	0.664	6.245
	DBP	6000	-0.028	3.560

within the range of 5 mmHg and 8 mmHg, respectively. For the BHS standard, performance accuracy is evaluated based on the percentage of cumulative error, categorized into three different grades (e.g., A, B, and C). These grades reflect the performance of the algorithm, as detailed in Table II with our evaluation outcome. To validate our results, we have conducted an evaluation on a total of 6000 subjects. Here, we have achieved a grade **A** in the BHS standard for both SBP and DBP, confirming the excellent performance of our methodology. The outcome of our proposed model is presented in Table III for the AAMI standard. The AAMI validation results indicate an ME±SD of 0.664±6.245 mmHg for SBP estimation and -0.028±3.560 mmHg for DBP estimation, both falling within the defined criteria.

IV. CONCLUSION

In this paper, we present a deep learning model for the estimation of BP using PPG signal acquired by a single sensor. The proposed featureless BP framework incorporates a data-driven end-to-end approach for automatic feature extraction during the training phase, eliminating complicated feature engineering. Data obtained from a large population with cardiovascular disease complications (the MIMIC-II dataset) shows the high accuracy of the model in noninvasive cuffless continuous BP monitoring. The model achieves MAE±SD of 4.852±6.245 mmHg and 2.937±3.560 for SBP and DBP, respectively. The performance of the AAMI and BHS international standards for noninvasive BP monitoring in wearable devices, paving the way for high-precision model that maps well onto low-power, portable medical devices.

ACKNOWLEDGMENT

This work was supported by InnoHK project at the Hong Kong Centre for Cerebro-cardiovascular Health Engineering (COCHE).

REFERENCES

[1] Liu et al, "Cuffless Blood Pressure Measurement using Smartwatches: A Large-scale Validation Study," *IEEE Journal of Biomedical and Health Informatics*, vol. 27, no. 9, pp. 4216-4227, May 2023.

[2] Ganti et al., "Wearable Cuff-less Blood Pressure Estimation at Home via Pulse Transit Time Cuffless BP measurement using a correlation study of pulse transient time and heart rate," *IEEE Journal of Biomedical and Health Informatics*, vol. 25, no. 6, June 2021.

[3] R. Mukkamala, et al., "Toward ubiquitous blood pressure monitoring via pulse transit time: theory and practice," *IEEE Trans. Biomed. Eng.*, vol. 62, no. 8, pp. 1879–1901, 2015.

[4] Young-Zoon Yoon, Jae Min Kang, Yongjoo Kwon, Sangyun Park, Seungwoo Noh, Youn-ho Kim, Jongae Park, and Sung Woo Hwang, "Cuff-less Blood Pressure Estimation using Pulse Waveform Analysis and Pulse Arrival Time," *IEEE Journal of Biomedical and Health Informatics*, vol. 22, no. 4, July 2018.

[5] Amirhossein Esmaili, Mohammad Kachuee, and Mahdi Shabany, "Nonlinear Cuffless Blood Pressure Estimation of Healthy Subjects Using Pulse Transit Time and Arrival Time," *IEEE Transactions on Instrumentation and Measurement*, vol. 66, no. 12, December 2017

[6] Sun, Yu, and Nitish Thakor, "Photoplethysmography revisited: from contact to noncontact, from point to imaging," *IEEE Transactions on Biomedical Engineering*, vol. 63, no. 3, pp. 463-477, 2015.

[7] Riaz, Farhan, et al. "Pervasive blood pressure monitoring using Photoplethysmogram (PPG) sensor," *Future Generation Computer Systems*, vol. 98, pp. 120-130, 2019.

[8] C. El-Hajj, and P. A. Kyriacou, "Cuffless blood pressure estimation from PPG signals and its derivatives using deep learning models," *Biomed. Signal Process Control,* vol. 70, 102984, 2021.

[9] Kachuee, Mohammad, et al. "Cuffless blood pressure estimation algorithms for continuous health-care monitoring." *IEEE Transactions on Biomedical Engineering*, vol. 64, no. 4, pp. 859-869, 2016.

[10] Navid Hasanzadeh, Mohammad Mahdi Ahmadi, and Hoda Mohammadzade, "Blood Pressure Estimation Using Photoplethysmogram Signal and Its Morphological Features," *IEEE Sensors Journal*, vol. 20, no. 8, April 2020

[11] Association for the Advancement of Medical Instrumentation, American national standards for electronic or automated sphygmomanometers. ANSI/AAMI SP 10-1987, 1987.

[12] E. O. Brien et al., "The british hypertension society protocol for the evaluation of automated and semi-automated blood pressure measuring devices with special reference to ambulatory systems," *J. Hypertens*., vol. 8, no. 7, pp. 607–619, 1990.

[13] Shresth Gupta, Anurag Singh, Abhishek Sharma, and Rajesh Kumar Tripathy, "Higher Order Derivative-Based Integrated Model for Cuff-Less Blood Pressure Estimation and Stratification Using PPG Signals," *IEEE Sensors Journal*, vol. 22, no. 22, November 2022

[14] X. Xing, and M. Sun, "Optical blood pressure estimation with photoplethysmography and FFT-based neural networks," *Biomed. Opt. Express*, vol. 7, no. 8, pp. 3007-3020, 2016.

[15] Pan Yao, Ning Xue, Siyuan Yin, Changhua You, Yusen Guo, Yi Shi, Tiezhu Liu, Lei Yao, Jun Zhou, Jianhai Sun, Cheng Dong, Chunxiu Liu, Ming Zhao, "Multi-Dimensional Feature Combination Method for Continuous Blood Pressure Measurement Based on Wrist PPG Sensor," *IEEE Journal of Biomedical and Health Informatics*, vol. 26, no. 8, August 2022.

[16] C, El-Hajj, and P. A. Kyriacou, "Deep learning models for cuffless blood pressure monitoring from PPG signals using attention mechanism," *Biomed. Signal Process. Control*, vol. 65, 102301, 2021.

[17] Sen Yang, Yaping Zhang, Siu-Yeung Cho, Ricardo Correia, and Stephen P. Morgan, "Non-invasive cuff-less blood pressure estimation using a hybrid deep learning model," *Optical and Quantum Electronics*, 53:93, 2021.

[18] Saeed, Mohammed, et al. "Multiparameter Intelligent Monitoring in Intensive Care II (MIMIC-II): a public-access intensive care unit database." *Critical care medicine*, vol. 39, no. 5, 952, 2011.

[19] Kingma, Diederik P., and Jimmy Ba. "Adam: A method for stochastic optimization." arXiv preprint arXiv:1412.6980 (2014).